
NIERT: Accurate Numerical Interpolation through Unifying Scattered Data Representations using Transformer Encoder

Shizhe Ding Dongbo Bu*

Key Lab of Intelligent Information Processing, Institute of Computing Technology, CAS
School of Computer Science and Tech., University of Chinese Academy of Sciences
dingshizhe15@mails.ucas.ac.cn, dbu@ict.ac.cn

Abstract

Numerical interpolation for scattered data aims to estimate values for target points based on those of some observed points. Traditional approaches produce estimations through constructing an interpolation function that combines multiple basis functions. These approaches require the basis functions to be pre-defined explicitly, thus greatly limiting their applications in practical scenarios. Recent advances exhibit an alternative strategy that learns interpolation functions directly from observed points using machine learning techniques, say deep neural networks. This strategy, although promising, cannot effectively exploit the correlations between observed points and target points as it treats these types of points separately. Here, we present a learning-based approach to numerical interpolation using encoder representations of Transformers (thus called NIERT). NIERT treats the value of each target point as a masked token, which enables processing target points and observed points in a unified fashion. By calculating the partial self-attention between target points and observed points at each layer, NIERT gains advantages of exploiting the correlations among these points and, more importantly, avoiding the unexpected interference of target points on observed points. NIERT also uses the pre-training technique to further improve its accuracy. On three representative datasets, including two synthetic datasets and a real-world dataset, NIERT outperforms the existing approaches, e.g., on the TFRD-ADlet dataset for temperature field reconstruction, NIERT achieves an MAE of 1.897×10^{-3} , substantially better than the transformer-based approach (MAE: 27.074×10^{-3}). These results clearly demonstrate the accuracy of NIERT and its potential to apply in multiple practical fields.

1 Introduction

Numerical interpolation for scattered data plays important and fundamental roles in a wide range of practical scenarios, including solving partial differential equations (PDEs) [1], temperature field reconstruction [2], time series interpolation [3, 4]. In meshfree PDE solvers, the interpolation error often leads to deviations in subsequent calculations, which seriously affects the solution’s accuracy [5]. In the task of temperature field reconstruction for micro-scale electronics, interpolation methods are used to obtain the real-time working environment of electronic components from limited measurements, and imprecise interpolation will significantly increase the cost of predictive maintenance [2]. Thus, accurate approaches to numerical interpolation are highly desirable.

*Corresponding author.

A large number of approaches have been proposed for interpolation of scattered data, which can be divided into two categories, namely, traditional non-learning based methods and recent learning-based methods. The typical traditional interpolation schemes construct the target function by a linear combination of basis functions [6]. These schemes require explicitly-defined basis functions to model the target function space, and various types of basis functions have been devised by algorithm designers to adapt to different scenarios. Nevertheless, such methods still suffer from limitations of high requirement of sufficient observed points, and the limited complexity of the target function.

Recent progress has exhibited an alternative strategy that uses neural networks to learn interpolation functions directly from the given observed points. For example, conditional neural processes (CNPs) [7] and their extensions [8–10] model the conditional distribution of regression functions given the observed points. In addition, Chen et al. [2] proposed to use vanilla Transformer [11] to solve interpolation task in temperature field reconstruction. All of these approaches use an “encoder-decoder” architecture, in which the encoder learns the representations of observed points while the decoder estimates values for target points. Intuitively, observed points and target points should be processed in a unified fashion because they are from the same domain. However, this architecture treats them separately and cannot effectively exploit the correlation between them.

Inspired by the recent advances of language/image models, especially BERT [12] and BEiT [13], we designed an approach to numerical interpolation that can effectively exploit the correlations between observed points and target points. Our approach is a learning-based approach using the encoder representations of Transformers (thus called NIERT). The key elements of NIERT include: *i*) the use of the mask mechanism, which enables processing target points and observed points in a unified fashion, *ii*) a novel partial self-attention model, which calculates attentions between target points and observed points at each layer, thus gaining the advantages of exploiting the correlations between these two types of points and, more importantly, avoiding the unexpected interference of target points on observed points simultaneously, and *iii*) the use of the pre-training technique, which further improves the interpolation accuracy of NIERT.

The main contributions of this study are summarized as follows.

1. We propose an accurate approach to numerical interpolation for scattered data. On representative datasets, including both synthetic and real-world datasets, our approach outperforms existing approaches. The experimental results demonstrate the potential of our approach in a wide range of application fields. The source code of NIERT will be released for open source use.
2. We propose a novel partial self-attention mechanism to make Transformer incorporated with strong inductive bias for interpolation tasks; i.e., it can effectively exploit the correlation among two types of points but simultaneously avoid the interference of one type of points onto the others.
3. We propose to use the pre-training technique to enhance interpolation approaches. When facing an interpolation task in a newly-appearing application field, we can benefit from the experience learned from low-cost synthesized interpolation tasks.

2 Related works

2.1 Traditional interpolation approaches for scattered data

Traditional interpolation approaches for scattered data use explicit basis functions to construct interpolation function, e.g., Lagrange interpolation, Newton interpolation [6], B-spline interpolation [14], Shepard’s method [15], Kriging [16], and radial basis function interpolation (RBF) [17, 18]. Among these approaches, the classical Lagrange interpolation, Newton interpolation and B-splines interpolation are usually used for univariate interpolation. Wang et al. [19] proposed a high order multivariate approximation scheme for scattered data sets, in which approximation error is represented with Taylor expansions at data points, and basis functions are determined through minimizing the squares of approximation error.

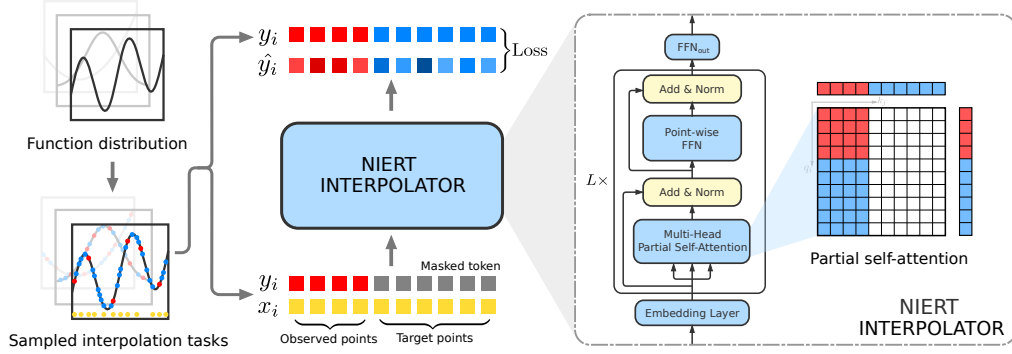


Figure 1: Overview of NIERT training process. Here, x_i represents the position of a point, and y_i represents its value. The predicted values of the point is denoted as \hat{y}_i . We prepare the training interpolation tasks by first sampling functions from a function distribution \mathcal{F} and then sampling observed points O and target points T on each function. NIERT trains an interpolator over this data. The partial self-attention mechanism facilitates exploiting the correlations between observed points and target points and avoiding the unexpected interference of target points on observed points

2.2 Neural network-based interpolation approaches

Equipped with deep neural networks, data-driven interpolation and reconstruction methods show great advantages and potential. For instance, convolutional neural networks (CNNs) have been applied in the interpolation tasks of single image super-resolution [20, 21], and recurrent neural networks (RNNs) and Transformers have been used for interpolation of sequences like time series data [4, 22].

Recently, Garnelo et al. [7] proposed to model the conditional distribution of regression functions given observed points. The proposed approach, conditional neural processes (CNPs), has shown increased estimation accuracy and generalizing ability. Kim et al. [8] designed an enhanced model, attentive neural processes (ANPs), with improved accuracy. Lee et al. [10] leveraged Bayesian last layer (BLL) [23] for faster training and better prediction. In addition, the bootstrap technique was also employed for further improvement [9]. To solve the interpolation task in 2D temperature field reconstruction, Chen et al. [2] proposed an Transformer-based approach, referred to as TFR-transformer, which can also be applied to solve interpolation tasks for scattered data with higher dimensions. Note that although TFR-transformer and our NIERT are both based on transformer, they are fundamentally different: *i*) TFR-transformer adopts an encoder-decoder structure and treats observed points and target points respectively, while NIERT adopts only a Transformer encoder (equipped with partial self-attention) to encode and learn correlation of the scattered data in a unified fashion; *ii*) TFR-transformer is trained by minimizing the prediction error of target points, while NIERT's training objective considers the prediction error of both observation points and target points.

2.3 Masked language/image models and the pre-training technique

The design of NIERT is also inspired by the recent advances in masked language/image models [12, 13, 24, 25] and pre-trained models for symbolic regression [26, 27]. The masked pre-trained models have been shown to be successful in learning representations of languages and images from large-scale data and improving the performance of downstream tasks. In addition, the mask mechanism makes the model able to reconstruct missing data from their context. Utilizing large-scale synthetic symbolic functions and sampled scattered data, Biggio et al. [26] and Valipour et al. [27] pre-trained Transformers to learn the map from scattered data to corresponding symbolic formulas. Different from these approaches, NIERT uses synthetic data to learn interpolating functions from scattered data numerically.

Algorithm 1 NIERT training process

Require: NIERT model M_θ with parameters θ , epoch number N , batch size B , domain X , function distribution \mathcal{F} and error metric function $\text{Error}(\cdot, \cdot)$

for k in $\{1..N\}$ **do**
 $J \leftarrow 0$
 for b in $\{1..B\}$ **do**
 $f, \{x_i\}_i \leftarrow$ sample a function and scatter points from \mathcal{F}, X
 $\{y_i\}_i \leftarrow$ calculate f on $\{x_i\}_i$
 $O, T \leftarrow$ split and mask scatter points with values $\{(x_i, y_i)\}_i$
 $\{\hat{y}_i\}_i \leftarrow M_\theta(O, T)$
 $J \leftarrow J + \sum_i \text{Error}(\hat{y}_i, y_i)$
 end for
 Compute the gradient $\nabla_\theta J$ and update θ
end for

3 Method

3.1 Overview of NIERT

In the study, we focus on the interpolation task that can be formally described as follows: We are given n observed points with known values $O = \{(x_i, y_i)\}_{i=1}^n$, and m target points with values to be determined, denoted as $T = \{x_i\}_{i=n+1}^{n+m}$. Here, $x_i \in X$ denotes position of a point, $y_i = f(x_i) \in Y$ denotes the value of a point, and $f: X \rightarrow Y$ denotes a function mapping positions to values. The function f is from a function distribution \mathcal{F} , which can be explicitly defined using a mathematical formula or implicitly represented using a set of scattered data in the form (x_i, y_i) . The goal of interpolation task is to accurately estimate the values $f(x)$ for each target point $x \in T$ according to the observed points in O .

Figure 1 depicts the schematic diagram of our NIERT approach. Briefly speaking, our approach employs a data-driven approach to numerical interpolation using encoder representations of Transformers. The main element of our approach is a neural interpolator that learns to estimate values for target points. The interpolator is featured by the characteristic that it treats the value of each target point as a masked token, thus enabling the unifying fashion to process both target points and observed points in the subsequent encoding and estimation procedures.

To suit the interpolation task, we design a *partial self-attention* mechanism: on one side, we calculate the attention between target points and observed points at each layer, which gains NIERT the advantage to effectively exploit the correlations between these two types of points. On the other side, the attention is a partial one as we do not consider the effects of a target point on all other points. This way, the unexpected interference of target points onto the observed points, and the interference among target points, are completely avoided.

The training process is depicted in Algorithm 1. Specifically, we prepare the training interpolation tasks by first sampling functions from a distribution \mathcal{F} and then sampling observed points O and target points T on each function. When training NIERT, we set the loss function as the error between the estimated values and the corresponding ground-truth. It should be pointed out that errors acquired on both observed points and target points are accounted into loss function.

3.2 Architecture of the NIERT interpolator

The neural interpolator in NIERT adopts the Transformer encoder framework; however, to suit the interpolation task, significant modifications and extensions were made in embedding, Transformer and output layers, which are described in details below.

Embedding with masked tokens: NIERT embeds both observed points and target points into the unified high-dimensional embedding space. As the position x of a data point and its value y are from different domains, we use two linear modules: Linear_x embeds the positions while Linear_y embeds the values.

It should be noted that for target points, their values are absent when embedding as they are to be determined. In this case, we use a masked token as substitutes, which is embedded as a trainable parameter MASK_y as performed in BERT [12]. This way, the interpolator processes both target points and observed points in a unifying fashion.

We concatenate the embeddings of position and value of a data point as the point’s embedding, denoted as h_i^0 , i.e.,

$$h_i^0 = \begin{cases} [\text{Linear}_x(x_i), \text{Linear}_y(y_i)], & \text{if } (x_i, y_i) \in O \\ [\text{Linear}_x(x_i), \text{MASK}_y], & \text{if } x_i \in T \end{cases}$$

Transformer layer with partial self-attention mechanism: NIERT feeds the embeddings of the points into a stack of L Transformer layers, producing encodings of these points as results. Each Transformer layer contains two subsequent sub-layers, namely, a multi-head self-attention module, and a point-wise fully-connected network. These sub-layers are interlaced with residual connections and layer normalization between them.

To avoid the unexpected interference of target points on observed points and target points themselves, NIERT replaces the original self-attention in Transformer layer with a *partial self-attention*, which calculates the feature of point i at the $l + 1$ -st layer as follows:

$$h^{l+1} = \text{LayerNorm}(\tilde{v}^l + \text{MLP}(\tilde{v}^l)),$$

$$\tilde{v}_i^l = \text{LayerNorm}\left(v_i^l + \sum_j w_{ij} \alpha_{ij}^l v_j^l\right)$$

where v_i^l and α_{ij}^l represent the value embedding and ordinary attention weights at the l -th layer as calculated in Transformer [11]. In this formula, we introduce a new term w_{ij} that represents the partial self-attention pattern, i.e.,

$$w_{ij} = \begin{cases} 1, & \text{if } (x_j, y_j) \in O \\ 0, & \text{if } x_j \in T \end{cases}.$$

By forcing the weight w_{ij} to be 0 for a target point i and any point j , we completely avoid the unexpected interference of target points on the other points.

Estimating values for target points: For each target point i , we estimate its value \hat{y}_i through feeding its features at the final Transformer layer into a fully connected feed-forward network, i.e.,

$$\hat{y}_i = \text{MLP}_{\text{out}}(h_i^L).$$

We calculate the error between the estimation and the corresponding ground-truth value, and compose the errors for all points into a loss function to be minimized.

3.3 Enhancing NIERT using pre-training technique

The interpolation functions from different applications usually differ greatly in their forms; however, the interpolation tasks might still share some common characteristics, say the correlation between observed points and target points. These common characteristics enable enhancing NIERT using the pre-training technique. Here, we pre-train NIERT using a synthetic dataset (see 4.1 for further details) and fine-tune it on other datasets in application fields.

4 Experiments and results

We evaluated NIERT and compared it with ten representative scattered data interpolation approaches on both synthetic and real-world datasets. We also examined the effects of the key elements of NIERT, including the partial self-attention, and the pre-training technique.

4.1 Experiment setting

The datasets, metrics and approaches for comparison are briefly described below. Further details of experiment settings are provided in Supplementary text.

Datasets: Three representative datasets in various application fields, including two synthetic datasets NeSymReS and TFRD-ADlet, and real-world dataset PhysioNet, are used for evaluation.

NeSymReS is a synthetic dataset for mathematical function interpolation, which is built using data generator proposed by Biggio et al. [26] and Lample and Charton [28]. We construct a function set with various dimensionality of data points, including 1D, 2D, 3D, and 4D. Scattered points in each instance are randomly sampled and divided into observed points and target points.

TFRD-ADlet [2] is a synthetic dataset for 2D temperature field reconstruction where each instance represents a simulated 2D temperature field containing several heat source components and a specific Dirichlet conditioned boundary. The goal of each task instance is to reconstruct the whole temperature field according to a limited number of observed points with measured temperature.

PhysioNet Challenge 2012 dataset [29] is a real world dataset collected from intensive care unit (ICU) records for time-series data interpolation. Each point in an instance represents a measurement at a specific time, where each measurement contains up to 37 physiological indices. Following the study [22], we randomly divided the points into observed points and target points by setting the ratio of observed points at five levels, i.e., 50%, 60%, 70%, 80%, and 90%. Note that this dataset is a representative of hard interpolation tasks due to the sparsity and irregularity of the records.

Pre-training dataset: In this study, NeSymReS dataset was used for pre-training NIERT to further improve its interpolation accuracy on TFRD-ADlet and PhysioNet dataset. For TFRD-ADlet dataset we directly use 2D TFRD-ADlet dataset for pre-training. As the PhysioNet dataset has a dimensionality of 37, we construct the pre-training instances by stacking random 37 functions from 1D TFRD-ADlet dataset and then sampling interpolation task instances.

Metrics: When evaluating NIERT and other interpolation approaches, the prediction error of target points are calculated as interpolation accuracy. For the NeSymReS and PhysioNet dataset, we adopted mean squared error (MSE) as the error metric. For TFRD-ADlet dataset, we use three error metrics: mean absolute error (MAE), MAE in component area (CMAE) and MAE at boundary (BMAE) following Chen et al. [2]. Accordingly, we use L_2 -form loss function for NeSymReS and PhysioNet dataset and L_1 -form loss function for TFRD-ADlet dataset for training.

Approaches for comparison: For NeSymReS dataset, we compared NIERT with six representative interpolation approaches, including RBF[30], MIR [19], CNP[7], ANP[8], BANP[9] and TFR-transformer [2]. For TFRD-ADlet we compared NIERT with CNP, ANP, BANP and TFR-transformer. For PhysioNet we compared NIERT with four approaches designed for time-series data interpolation, including RNN-VAE [31], L-ODE-RNN [32], L-ODE-ODE[33], and mTAND-Full[22].

4.2 Interpolation accuracy on synthetic and real-world datasets

For each instance of the test datasets, we applied the trained NIERT to estimate values for the target points. We calculate the errors between the estimation and the ground-truth as interpolation accuracy.

Interpolation approach	MSE ($\times 10^{-5}$) on NeSymReS test set			
	1D	2D	3D	4D
RBF	215.439	347.060	443.094	327.775
MIR	67.281	274.601	448.933	342.997
CNP	67.176	248.668	392.348	314.311
ANP	34.558	140.005	206.699	164.751
BANP	14.913	84.187	143.518	140.288
TFR-transformer	15.556	58.569	99.986	90.579
NIERT	8.964	45.319	77.664	72.025

Interpolation approach	Evaluation criteria ($\times 10^{-3}$)		
	MAE	CMAE	BMAE
CNP	96.674	109.419	56.939
ANP	54.684	62.511	26.524
BANP	28.671	29.450	19.984
TFR-transformer	27.074	29.772	18.835
NIERT	3.473	3.947	2.467
NIERT w/ pretraining	1.897	1.971	1.246

Table 1: Interpolation accuracy of NIERT and the existing approaches on NeSymReS test dataset

Table 2: Interpolation accuracy of NIERT and the existing approaches over the TFRD-ADlet dataset

Accuracy on the NeSymReS dataset: As shown in Table 1, on the 1D NeSymReS testset, RBF shows the largest interpolation error (MSE: 215.439). MIR, another approach using explicit basis functions, also shows a high interpolation error of 67.281. In contrast, BANP and TFR-transformer, which use neural networks to learn interpolation, show relatively lower errors (MSE: 14.913, 15.556). Compared with these approaches, our NIERT approach achieves the best interpolation accuracy (MSE: 8.964). Table 1 also demonstrates the advantage of NIERT over the existing approach on the 2D, 3D, and 4D instances.

Interpolation approach	Ratio of observed points				
	50%	60%	70%	80%	90%
RNN-VAE	13.418±0.008	12.594±0.004	11.887±0.005	11.133±0.007	11.470±0.006
L-ODE-RNN	8.132±0.020	8.140±0.018	8.171±0.030	8.143±0.025	8.402±0.022
L-ODE-ODE	6.721±0.109	6.816±0.045	6.798±0.143	6.850±0.066	7.142±0.066
mTAND-Full	4.139±0.029	4.018±0.048	4.157±0.053	4.410±0.149	4.798±0.036
NIERT	2.868±0.021	2.811±0.032	2.656±0.041	2.598±0.078	2.709±0.157
NIERT w/ pretraining	2.831±0.021	2.771±0.019	2.641±0.052	2.539±0.085	2.596±0.159

Table 3: The relationship between interpolation accuracy (measured using MSE, $\times 10^{-3}$) and the ratio of observed points. Here, we use the PhysioNet dataset as representatives

Note that the number of observed points varies greatly in test instances, making the average interpolation error calculated over all test instances insufficient to measure interpolation performance. Therefore, we further divide test instances into subsets according to the number of observed points. As shown in Figure 2, as the number of observed points increases, the interpolation error decreases as expected. In addition, the relative advantages of these approaches vary with the number of observed points, e.g., CNP is better than RBF and MIR initially but finally becomes worse as the number of observed points increases. Among all approaches, NIERT stably shows the best performance over all test subsets, regardless of the number of observed points.

Accuracy on the TFRD-ADlet dataset: As shown in Table 2, CNP, although employing the neural network technique, still performs poorly with MAE as high as of 96.674. In contrast, NIERT achieves the lowest interpolation error (MAE: 3.473), which is over one order of magnitude lower than CNP, ANP, BANP and TFR-transformer. Moreover, when enhanced with the pre-training technique, NIERT can further decrease its interpolation MAE to be 1.897. Besides MAE, other metrics, say CMAE and BMAE, also show the superior of NIERT over the existing approaches (Table 2).

Accuracy on the PhysioNet dataset: Table 3 suggests that on the PhysioNet dataset, NIERT also outperforms the existing approaches, e.g., when controlling the ratio of observed points to be 50%, NIERT achieves an average MSE ($\times 10^{-3}$) of 2.868, significantly lower than RNN-VAE (13.418), L-ODE-RNN (8.132), L-ODE-ODE (6.721) and mTAND-Full (4.139). Again, NIERT with the pre-training technique shows better performance. The advantages of NIERT hold across various settings of the ratio of the observed points.

Taken together, these results clearly demonstrate the power of NIERT for numerical interpolation in multiple application fields, including interpolating the scattered data generated using mathematical functions, reconstructing temperature fields, and interpolating time-series data.

4.3 Case studies of interpolation results

To further understand the advantages of NIERT, we carried out case studies through visualizing the observed points, the reconstructed interpolation functions and the interpolation errors in this subsection. More visualized cases are put in the Supplementary material.

Figure 3 show a 2D instance in the NeSymReS test set, respectively. As illustrated by these two figures, RBF performs poorly in the application scenario with sparse observed data. In addition, RBF and MIR, especially ANP, cannot accurately predict values for the target points that fall out of the range restricted by observed points. The CNP approach can only learn the rough trend stated by the observed points, thus leading to significant errors. In contrast, BANP, TFR-transformer and NIERT can accurately estimate values for target points within considerably large range, and compared with BANP and TFR-transformer, NIERT can produce more accurate results.

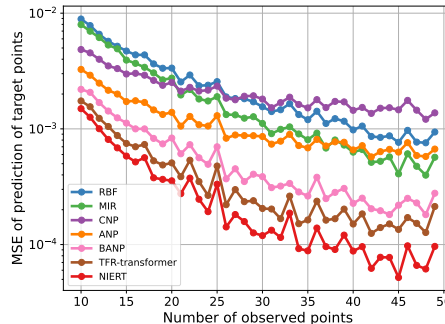


Figure 2: The relationship between the interpolation accuracy and the number of observed points. Here we use the 2D instances in the NeSymReS test dataset as representatives

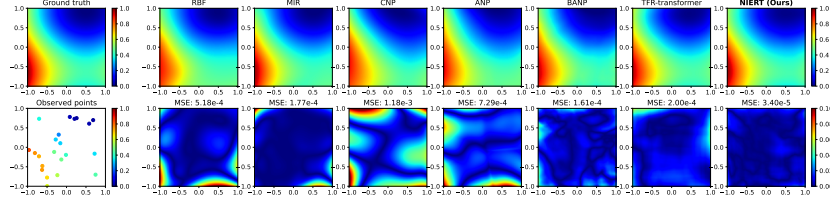


Figure 3: An example of 2D interpolation task extracted from NeSymReS test set. The up-left figure shows the ground-truth function while the bottom-left figure shows the 22 observed points. The interpolation functions reported by NIERT and the existing approaches are listed on the top panel with their differences with the ground-truth are list below

Figure4 shows an instance of temperature field reconstruction extracted from TFRD-ADlet. From this figure, we can observe that when using pre-training technique, NIERT further improves its interpolation accuracy in the whole area.

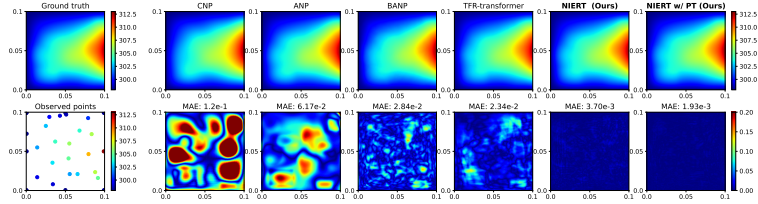


Figure 4: An example of temperature field reconstruction task extracted from TFRD-ADlet test set. The up-left figure shows the ground-truth temperature field while the bottom-left figure shows the 32 observed points. The reconstructed results reported by NIERT and the existing approaches are listed on the top panel with their differences with the ground-truth temperature field are list below

4.4 Contribution analysis of observed points for interpolation

An idealized interpolation approach is expected to effectively exploit all observed points with appropriate consideration of relative positions among observed points and target points as well. To examine this issue, we visualized the attention weight of each observed point to all target points. These attention weights provide an intuitive description of the contribution by observed points.

As shown in Figure 5, when using TFR-transformer, the contributions by observed points are considerably imbalanced: on one side, some observed points might affect their neighboring target points in a large region; on the other side, the other observed points have little contributions to interpolation. In contrast, when using NIERT, contributions by an observed point are much more local and thus targeted. More importantly, all observed points have contributions to interpolation.

These results demonstrate that NIERT can exploit the correlation between observed points and target points more effectively.

4.5 Ablation study

The effects of partial self-attention: For a specific interpolation task, the interpolation function is determined by the observed points only. Thus, an idealized encoding of observed points should not be affected by target points. To investigate the affects of target points, we evaluated NIERT on the test sets with various number of target points. Here, we compared two variants of NIERT, one with partial self-attention, and the other with vanilla self-attention. Both of these two variants were trained using the same training sets (the number of target points varies within [206, 246]).

As illustrated by Figure 6, the variant with vanilla self-attention shows poor performance for the tasks with few target points, say less than 64 target points. In contrast, the variant with partial self-attention always performs stably without significant changes of accuracy.

The results clearly demonstrate that the partial self-attention mechanism allows NIERT to be free from the unexpected affects by the target points.

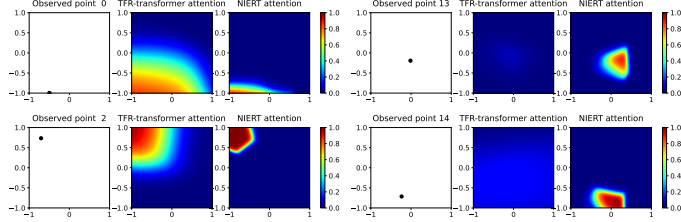


Figure 5: Contributions by observed points for interpolation. The 2D instance is same to that used in Figure 3. We randomly select 4 observed points and extract their attention weights from the final attention layer of NIERT and TFR-transformer. These attention weights provide an intuitive description of the contribution by observed points. The contributions by other 18 observed points are shown in Supplementary material

The effects of pre-training technique: To investigate the effects of the pre-training technique, we show in Figure 7 the training process of two versions of NIERT, one without pre-training technique, and the other enhanced with pre-training. As depicted by the figure, even at the first epoch, the pre-trained NIERT shows a sufficiently high interpolation accuracy, which is comparable with the fully-trained BANP and TFR-transformer. Moreover, the performance of the pre-trained NIERT improves in roughly the same convergence speed to the original NIERT. At the final epoch, the pre-trained NIERT decreases the interpolation error to be nearly half of that of the original NIERT.

These results clearly suggest that the experience learned by NIERT from the interpolation task in one application field has potential to be transferred to the interpolation tasks in other application fields.

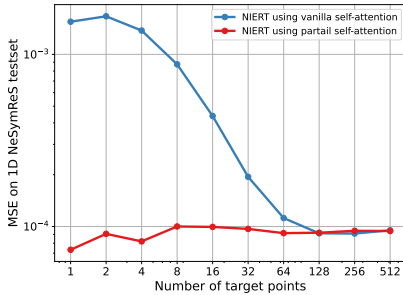


Figure 6: The robustness of NIERT to the number of target points. Here, two variants of NIERT are trained on 1D NeSymReS dataset

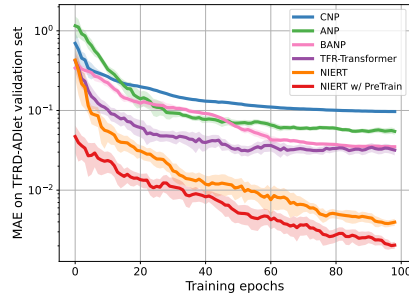


Figure 7: The convergence of NIERT, NIERT with pre-training, and the existing approaches. Here, models are trained on TFRD-ADlet dataset

5 Discussion and conclusion

We present in the study an accurate approach to numerical interpolation for scattered data. The specific features of our NIERT approach are highlighted by the full exploitation of the correlation between observed points and target points through unifying scattered data representation. At the same time, the use of partial self-attention mechanism can effectively avoid the interference of target points onto the observed points. The enhancement with pre-training technique is another special feature of NIERT. The advantages of NIERT in interpolation accuracy have been clearly demonstrated by experimental results on both synthetic and real-world datasets.

The current version of NIERT has a computational complexity of $O(n(m+n))$, thus cannot handle the interpolation tasks with extremely large amounts of observed points due to the limitations of GPU memory size. Compared with the lightweight traditional methods, our NIERT approach has a much larger model with expensive computation to learn complex function distribution, which limits its application in cost sensitive scenarios. How to reduce the memory requirement and computational cost is one of the future works. Additionally, it is interesting to combine NIERT and the traditional approaches based on basis functions to yield an approach with both high accuracy and interpretability.

We expect NIERT, with extensions and modifications, to greatly facilitate numerical interpolations in a wide range of engineering and science fields.

Acknowledgements

We would like to thank the National Key Research and Development Program of China (2020YFA0907000), and the National Natural Science Foundation of China (32271297, 62072435, 31770775, 31671369) for providing financial supports for this study and publication charges.

References

- [1] Richard Franke and Gregory M Nielson. Scattered data interpolation and applications: A tutorial and survey. *Geometric Modeling*, pages 131–160, 1991.
- [2] Xiaoqian Chen, Zhiqiang Gong, Xiaoyu Zhao, Weien Zhou, and Wen Yao. A Machine Learning Modelling Benchmark for Temperature Field Reconstruction of Heat-Source Systems. *arXiv preprint arXiv:2108.08298*, 2021.
- [3] Mathieu Lepot, Jean-Baptiste Aubin, and François HLR Clemens. Interpolation in time series: An introductory overview of existing methods, their performance criteria and uncertainty assessment. *Water*, 9(10):796, 2017.
- [4] Satya Narayan Shukla and Benjamin M Marlin. Interpolation-prediction networks for irregularly sampled time series. *arXiv preprint arXiv:1909.07782*, 2019.
- [5] GR3543275 Liu. An overview on meshfree methods: for computational solid mechanics. *International Journal of Computational Methods*, 13(05):1630001, 2016.
- [6] Michael T Heath. *Scientific Computing: An Introductory Survey, Revised Second Edition*. Society for Industrial and Applied Mathematics, revised 2nd edition edition, 2018.
- [7] Marta Garnelo, Dan Rosenbaum, Christopher Maddison, Tiago Ramalho, David Saxton, Murray Shanahan, Yee Whye Teh, Danilo Rezende, and S. M. Ali Eslami. Conditional Neural Processes. In Jennifer Dy and Andreas Krause, editors, *Proceedings of the 35th International Conference on Machine Learning*, volume 80 of *Proceedings of Machine Learning Research*, pages 1704–1713. PMLR, 10–15 Jul 2018.
- [8] Hyunjik Kim, Andriy Mnih, Jonathan Schwarz, Marta Garnelo, Ali Eslami, Dan Rosenbaum, Oriol Vinyals, and Yee Whye Teh. Attentive Neural Processes. In *International Conference on Learning Representations*, 2019.
- [9] Juho Lee, Yoonho Lee, Jungtaek Kim, Eunho Yang, Sung Ju Hwang, and Yee Whye Teh. Bootstrapping neural processes. In H. Larochelle, M. Ranzato, R. Hadsell, M.F. Balcan, and H. Lin, editors, *Advances in Neural Information Processing Systems*, volume 33, pages 6606–6615. Curran Associates, Inc., 2020.
- [10] Byung-Jun Lee, Seunghoon Hong, and Kee-Eung Kim. Residual neural processes. In *Proceedings of the AAAI Conference on Artificial Intelligence*, volume 34, pages 4545–4552, 2020.
- [11] Ashish Vaswani, Noam Shazeer, Niki Parmar, Jakob Uszkoreit, Llion Jones, Aidan N Gomez, Łukasz Kaiser, and Illia Polosukhin. Attention is all you need. In *Advances in Neural Information Processing Systems*, pages 5998–6008, 2017.
- [12] Jacob Devlin, Ming-Wei Chang, Kenton Lee, and Kristina Toutanova. BERT: Pre-training of deep bidirectional transformers for language understanding. *arXiv preprint arXiv:1810.04805*, 2018.
- [13] Hangbo Bao, Li Dong, and Furu Wei. BEiT: BERT Pre-Training of Image Transformers. *arXiv preprint arXiv:2106.08254*, 2021.
- [14] Charles A Hall and W Weston Meyer. Optimal error bounds for cubic spline interpolation. *Journal of Approximation Theory*, 16(2):105–122, 1976.

- [15] William J Gordon and James A Wixom. Shepard’s method of “metric interpolation” to bivariate and multivariate interpolation. *Mathematics of computation*, 32(141):253–264, 1978.
- [16] Hans Wackernagel. *Multivariate geostatistics: an introduction with applications*. Springer Science & Business Media, 2003.
- [17] Michael JD Powell. Radial basis functions for multivariable interpolation: a review. *Algorithms for approximation*, 1987.
- [18] Bengt Fornberg and Julia Zuev. The Runge phenomenon and spatially variable shape parameters in RBF interpolation. *Computers & Mathematics with Applications*, 54(3):379–398, 2007.
- [19] Qiqi Wang, Parviz Moin, and Gianluca Iaccarino. A high order multivariate approximation scheme for scattered data sets. *Journal of Computational Physics*, 229(18):6343–6361, 2010.
- [20] Ying Tai, Jian Yang, and Xiaoming Liu. Image super-resolution via deep recursive residual network. In *Proceedings of the IEEE conference on computer vision and pattern recognition*, pages 3147–3155, 2017.
- [21] Juncheng Li, Zehua Pei, and Tiejong Zeng. From Beginner to Master: A Survey for Deep Learning-based Single-Image Super-Resolution. *arXiv preprint arXiv:2109.14335*, 2021.
- [22] Satya Narayan Shukla and Benjamin Marlin. Multi-Time Attention Networks for Irregularly Sampled Time Series. In *International Conference on Learning Representations*, 2021.
- [23] Noah Weber, Janez Starc, Arpit Mittal, Roi Blanco, and Lluís Màrquez. Optimizing over a bayesian last layer. In *NeurIPS workshop on Bayesian Deep Learning*, 2018.
- [24] Tom Brown, Benjamin Mann, Nick Ryder, Melanie Subbiah, Jared D Kaplan, Prafulla Dhariwal, Arvind Neelakantan, Pranav Shyam, Girish Sastry, Amanda Askell, Sandhini Agarwal, Ariel Herbert-Voss, Gretchen Krueger, Tom Henighan, Rewon Child, Aditya Ramesh, Daniel Ziegler, Jeffrey Wu, Clemens Winter, Chris Hesse, Mark Chen, Eric Sigler, Mateusz Litwin, Scott Gray, Benjamin Chess, Jack Clark, Christopher Berner, Sam McCandlish, Alec Radford, Ilya Sutskever, and Dario Amodei. Language Models are Few-Shot Learners. In H. Larochelle, M. Ranzato, R. Hadsell, M. F. Balcan, and H. Lin, editors, *Advances in Neural Information Processing Systems*, volume 33, pages 1877–1901. Curran Associates, Inc., 2020.
- [25] Kaiming He, Xinlei Chen, Saining Xie, Yanghao Li, Piotr Dollár, and Ross Girshick. Masked autoencoders are scalable vision learners. *arXiv preprint arXiv:2111.06377*, 2021.
- [26] Luca Biggio, Tommaso Bendinelli, Alexander Neitz, Aurelien Lucchi, and Giambattista Parascandolo. Neural Symbolic Regression that Scales. In *International Conference on Machine Learning*, pages 936–945. PMLR, 2021.
- [27] Mojtaba Valipour, Bowen You, Maysum Panju, and Ali Ghodsi. SymbolicGPT: A Generative Transformer Model for Symbolic Regression. *arXiv preprint arXiv:2106.14131*, 2021.
- [28] Guillaume Lample and François Charton. Deep learning for symbolic mathematics. *arXiv preprint arXiv:1912.01412*, 2019.
- [29] Ikaro Silva, George Moody, Daniel J Scott, Leo A Celi, and Roger G Mark. Predicting in-hospital mortality of icu patients: The physionet/computing in cardiology challenge 2012. In *2012 Computing in Cardiology*, pages 245–248. IEEE, 2012.
- [30] Pauli Virtanen, Ralf Gommers, Travis E. Oliphant, Matt Haberland, Tyler Reddy, David Cournapeau, Evgeni Burovski, Pearu Peterson, Warren Weckesser, Jonathan Bright, Stéfan J. van der Walt, Matthew Brett, Joshua Wilson, K. Jarrod Millman, Nikolay Mayorov, Andrew R. J. Nelson, Eric Jones, Robert Kern, Eric Larson, C J Carey, İlhan Polat, Yu Feng, Eric W. Moore, Jake VanderPlas, Denis Laxalde, Josef Perktold, Robert Cimrman, Ian Henriksen, E. A. Quintero, Charles R. Harris, Anne M. Archibald, Antônio H. Ribeiro, Fabian Pedregosa, Paul van Mulbregt, and SciPy 1.0 Contributors. SciPy 1.0: Fundamental Algorithms for Scientific Computing in Python. *Nature Methods*, 17:261–272, 2020. doi: 10.1038/s41592-019-0686-2.

- [31] Junyoung Chung, Caglar Gulcehre, KyungHyun Cho, and Yoshua Bengio. Empirical evaluation of gated recurrent neural networks on sequence modeling. *arXiv preprint arXiv:1412.3555*, 2014.
- [32] Ricky T. Q. Chen, Yulia Rubanova, Jesse Bettencourt, and David Duvenaud. Neural Ordinary Differential Equations. *Advances in Neural Information Processing Systems*, 2018.
- [33] Yulia Rubanova, Ricky T. Q. Chen, and David K Duvenaud. Latent Ordinary Differential Equations for Irregularly-Sampled Time Series. In H. Wallach, H. Larochelle, A. Beygelzimer, F. d'Alché-Buc, E. Fox, and R. Garnett, editors, *Advances in Neural Information Processing Systems*, volume 32. Curran Associates, Inc., 2019.

A Broader impact

Numerical interpolation is fundamental in numerical methods and it has been widely used in a large variety of practical scenarios. In this study, our NIERT approach has been verified in temperature-field reconstruction and time-series data imputation, which shows its potential in weather prediction, industrial environmental monitoring.

B Theoretical explanation of NIERT

Here we provide a theoretical explanation of NIERT to explain why NIERT performs excellent in tasks of scattered data interpolation. This explanation is based on the tight connection between the core mechanism of NIERT, namely partial self-attention mechanism, and classical RBF interpolation algorithm.

Given n observed points, RBF interpolation formulates the interpolant as

$$\hat{f}(x) = \sum_{j=1}^n \lambda_j \phi(x, x_j)$$

where $\phi(x, x_j)$ is the radial basis function related to the observed point x_j and λ_j is the coefficient to be determined. In partial self-attention layer of NIERT, a point x_i 's representation \tilde{v}_i is computed by

$$\tilde{v}_i = \sum_{j=1}^n \alpha(q_i, k_j) v_j$$

where $\alpha(q_i, k_j)$ is the normalized attention weight function. $\alpha(q_i, k_j)$ models the correlation between any query vector q_i (q_i is related to an observed point or a target point) and key vector k_j (k_j is related to an observed point x_j).

Obviously, we can regard partial self-attention as a general form of RBF interpolant by corresponding $\alpha(\cdot, \cdot)$ to $\phi(\cdot, \cdot)$ and v_j to λ_j . Based on neural networks, $\alpha(\cdot, \cdot)$ and v_j is learnable. Thus by adding other appropriate modules and mechanisms, such as MLPs, skip connection, layer normalization, multi-head mechanisms, and applying supervised training, it is promising to get a high-accuracy neural interpolator, which adapts to a certain function distribution.

C Implementation and experiment details

We provide the details of implementation and experiments in this section and deposit source code of NIERT at <https://anonymous.4open.science/r/NIERT-2BCF>.

On NeSymReS dataset:

Table 4 lists the hyper-parameters of NIERT when running on the NeSymReS dataset. For fair comparison, we set up the TFR-transformer with the same H and d_{model} , and the number of its encoder layers is set to 5 and that of its decoder is set to 1 following [2], which shows its best performance. We trained NIERT and the neural approaches for comparison on two NVIDIA GeForce

Parameter name	Symbol	Value
Number of layers	L	6
Hidden dimension	d_{model}	512
Number of heads	H	8
x 's embedding dimension	d_{xemb}	$16 \times d_x$
y 's embedding dimension	d_{yemb}	16

Table 4: Hyper-parameters of NIERT in experiments on NeSymReS dataset

RTX 3090 GPUs for 160 epochs with a batch size of 128. Adam optimizer with a learning rate of 1.0×10^{-4} and no schedules are performed for parameters optimization.

On TFRD-ADlet and PhysioNet dataset:

For experiments on TFRD-ADlet and PhysioNet dataset, we use the NIERT implementation whose hyper-parameters are listed in Table 5. The pre-trained NIERT also has the same hyper-parameters. Also, for fair comparison, we set up the TFR-transformer with the same H and d_{model} , and the number of its encoder layers is set to 2 and that of its decoder is set to 1.

Parameter name	Symbol	Value
Number of layers	L	3
Hidden dimension	d_{model}	128
Number of heads	H	4
x 's embedding dimension	d_{xemb}	32
y 's embedding dimension	d_{yemb}	16

Table 5: Hyper-parameters of NIERT in experiments on TFRD-ADlet dataset

Parameter name	Symbol	Value
Number of layers	L	3
Hidden dimension	d_{model}	128
Number of heads	H	4
x 's embedding dimension	d_{xemb}	16
y 's embedding dimension	d_{yemb}	592

Table 6: Hyper-parameters of NIERT in experiments on PhysioNet dataset

For experiments on TFRD-ADlet dataset, we trained NIERT and the approaches for comparison on one NVIDIA GeForce RTX 3090 GPU for 100 epochs with a batch size of 5. Adam optimizer with a learning rate of 5.0×10^{-4} with a decay rate of 0.97 is performed. For experiments on PhysioNet dataset, we trained NIERT on one NVIDIA GeForce RTX 3090 GPU for 160 epochs with a batch size of 32. Adam optimizer with a learning rate of 5.0×10^{-4} and with a decay rate of 0.97 is performed.

Pre-trained NIERT on 2D NeSymReS is used to fine-tune on TFRD-ADlet dataset. To deal with the problem that the data distribution is too different between NeSymReS data and temperature field in TFRD-ADlet, we simply normalize the data of temperature field to the value range of 2D NeSymReS data before fine-tuning.

To apply NIERT on PhysioNet dataset in which each instance has so many dependent variables with a number of 37, we increase the number of MLPs for dependent variables to 37 in the embedding layer to embed them separately. The pre-training instances for these tasks are correspondingly different. For convenience, we stack 37 random 1D functions in NeSymReS dataset as an instance for pre-training. Although the data generated using such construction method is considerable different from PhysioNet data, we still observe that pre-training technique improves the interpolation accuracy as shown in Table 3.

D Dataset details

We evaluated NIERT approach using three datasets, including two synthetic datasets NeSymReS and TFRD-ADlet, and a real-world dataset PhysioNet, which are described in detail as below.

D.1 Synthetic dataset I: NeSymReS

We used the NeSymReS² dataset to test the performance of NIERT for mathematical function interpolation. This dataset was constructed following Biggio et al. [26] with only slight modification for the sake of numerical interpolation. For clarity, we put the details of construction procedure in the next subsection D.2, and list the summarized characteristics of this dataset as follows.

Instance construction: We randomly sampled N points from $X = [-1, 1]^{d_x}$ (d_x represents the point dimensionality) and calculate the values for these points with a mathematical function f . From these points, we randomly picked n points as observed points and used the left-over as target points. In the study, we chose different d_x for constructing datasets, including 1D, 2D, 3D, and 4D. For 1D NeSymReS dataset, we set the scattered points number N as 256. For 2D/3D/4D NeSymReS dataset, we set N as 512. We control observed points number n within the range of [5, 50].

Training set and test set: Each instance in training or test set was built using a mathematical function f . These functions were generated using a function sampler as performed in Ref. [26] (see further details in Supplementary text). During the training process, 1 million instances are dynamically

²Built based on <https://github.com/SymposiumOrganization/NeuralSymbolicRegressionThatScales>.

sampled at each epoch as training set. We used the L_2 -form loss function for this dataset. We also generated 12000 instances and used them as test set.

Dimensionality of points: We evaluated NIERT using scatter data with various dimensionality, including 1D, 2D, 3D, and 4D.

Approaches for comparison: We compared NIERT with five representative interpolation approaches, including radial basis function (RBF)[17, 18], MIR [16], conditional neural process (CNP)[7], attentive neural process (ANP)[8] and TFR-transformer [2]. Among these approaches, RBF and MIR are classical approaches that use explicit basis functions, while CNP, ANP and TFR-transformer use neural networks to learn how to interpolate.

D.2 NeSymReS dataset construction details

Following the study of Biggio et al. [26], firstly, we generate equation *skeletons* which is refer to the symbolic equation where numerical constants are replaced by placeholders [26]. Each equation skeleton has the configured number (d_x) of independent variables symbols. For example, $y = \sin(C_1x_1) + C_2x_2^2$ is a possible generated equation skeleton which includes constants placeholders C_1 and C_2 and two variables x_1 and x_2 . Such equation skeletons are considered expression trees during generation. Each randomly-generated expression tree has up-to 5 non-leaf nodes, i.e. function operators. Unnormalized weighted distribution shown in Table 7 is used for sampling each non-leaf node. Each leaf node has a probability of 0.8 of being an independent variable and 0.2 of being an integer. Different from [26] using almost all elementary functions symbols including discontinuous ones like \ln , \arcsin , \tan for symbolic regression tasks, we only use the operators listed in Table 7 which guarantee that the generated function is continuous in the whole domain $X = [-1, 1]^{d_x}$, to make it more suitable for interpolation tasks.

Operator	+	×	-	. ²	. ³	exp	sin	cos
Unnormalized probability	10	10	5	4	2	4	4	4

Table 7: Operator and corresponding un-normalized probabilities during the generating process of mathematical functions in NeSymReS dataset

Secondly, constants values are independently sampled from a uniform distribution $\mathcal{U}(1, 5)$ and we get a set of completely-defined mathematical-expression functions. Then we normalize those functions to make their values range in $[0, 1]$ and multiply it with a random number range $[0.9, 1]$ to produce diversity.

After those completely-defined functions obtained, we sample interpolation task for each function by randomly sampling a set of support points $\{x_i\}_i$ in X , evaluating the function and get the corresponding $\{y_i\}_i$, and then splitting those data points into a observed points set and a target points set. 512 scatter points are sampled using each function, of which a random number (ranging in $[5, 50]$) of points are set up as the observed points and the rest are set up as the target points.

During the generation of interpolation tasks, results with invalid values (NaN or inf) are removed. For d_x in configurations $\{1, 2, 3, 4\}$, we generate datasets separately and use them for training and testing. In particular, when d_x is configured, we generate 150 equation skeletons set for testing and 1 million skeletons set for training. Each skeleton in the training set existing in the test set has been removed. At training time, interpolation tasks are sampled using equation skeletons from the training set in real time. At testing time, we use an interpolation task set containing 10000 instances, which are generated by the testing skeletons set.

D.3 Synthetic dataset II: TFRD-ADlet

We use the TFRD-ADlet³ dataset to test the performance of NIERT for 2D temperature field reconstruction. This dataset simulates the temperature field of mechanical devices in a high-fidelity fashion[2]. The characteristics of this dataset are summarized as follows. *Instance construction:* Each instance has 200×200 regular grid points that represent the temperature field in a $0.1m \times 0.1m$

³TFRD-Alet is downloadable at <https://pan.baidu.com/s/14BipTer1fkilbRjrQNbKiQ>, password: 'tfrd'.

square area. Among these grid points, 32 points have their temperate known and used as observed points. The other 3968 points are used as target points.

Training set and test set: We have a total of 10,000 training instances and 10,000 test instances. For the sake of fair comparison, we also use L_1 -form loss function for this dataset as performed in Ref. [2].

Dimensionality of points: The grid points are in a 2D plane.

Approaches for comparison: For this dataset, we compared NIERT with three neural network-based interpolation approaches, including conditional neural process (CNP)[7], attentive neural process (ANP)[8] and TFR-transformer [2]. We also compared NIERT with its enhanced version that was pre-trained using the NeSymReS dataset.

D.4 Real-world dataset: PhysioNet

We use the PhysioNet⁴ dataset, excerpted from the PhysioNet Challenge 2012 [29], to test the performance of NIERT for time-series data interpolation. This real-world dataset were collected from intensive care unit (ICU) records. It should be pointed out that this dataset is a representative of hard interpolation tasks due to the sparsity and irregularity of the records.

Instance construction: Each instance consists of multiple points, each of which represents a measurement of a patient at a specific time. Following the study in Ref. [22], we randomly divided the points into observed points and target points. We also set the ratio of observed points at five levels, i.e., 50%, 60%, 70%, 80%, and 90%, and evaluated NIERT using the thus-acquired datasets.

Training set and test set: We randomly divided the 8,000 instances acquired from the PhysioNet Challenge 2012 into training set and test set with a ratio of 4:1. For the sake of fair comparison, we use L_2 -form loss function for this dataset as performed in Ref. [22].

Dinsionality of points: Each point in an instance represents a measurement at a specific time and each measurement contains up to 37 physiological indices; thus, the independent variable x is 1D while the dependent variable y has a dimensionality of 37.

Approaches for comparison: On this dataset, we compared NIERT with four representative approaches designed for time-series data interpolation, including RNN-VAE [31], L-ODE-RNN [32], L-ODE-ODE[33], and mTAND-Full[22]. The details of these approaches are provided in Supplementary text. We also compared NIERT with its enhanced version that was pre-trained using the NeSymReS dataset.

E Approaches for comparison

Radial basis function (RBF) RBF is one of the most commonly-used scattered data interpolation methods. It adopts a specific type of radial basis functions on observed points and uses their linear combination to represent the target function. We use the RBF interpolation implementation in SciPy [30] and multiquadric function as basis function type for the experiments.

MIR MIR⁵ is another multivariate interpolation and regression method for scattered data sets proposed by [19]. MIR represents the approximation error with Taylor expansions and minimizes the approximation error to find the basis functions.

Conditional nerual process (CNP) CNP proposed by [7] is an neural model able to learn to predict distributions of target points values given a series of observed points. In order to fully verify the accuracy of interpolation, we let CNP to predict the values of target only and the training criteria function is set to be the prediction error of values of target points in the experiments.

Attentive nerual process (ANP) ANP [8] leverages attention mechanism in CNP and improves the prediction performance. In the experiments, the criteria function are fixed as same as CNP above.

⁴PhysioNet is downloadable at <https://physionet.org/content/challenge-2012/1.0.0/>.

⁵MIR's implementation can be found at <http://web.mit.edu/qiqi/www/mir/>

Bootstrapping attentive neural process (BANP) BANP [9] employs bootstrap technique to further improve the performance of ANP. In the experiments, the criteria function are fixed as same as CNP and ANP above.

TFR-Transformer Transformer [8] is originally proposed to solve tasks in natural language processing. [2] adopts Transformer in 2-dimensional temperature field reconstruction using scattered observations. Compared with vanilla transformer, TFR-Transformer removes positional encoding, encodes the observations using encoder, using cross-attention mechanism between observations’ encoding and target points to represents targets’ features at decoder, and using a MLP to map targets’ features to values.

RNN-VAE RNN-VAE is a VAE-based model where the encoder and decoder are standard RNN models. Gated Recurrent Unit (GRU) [31] module is configured as the recurrent network.

L-ODE-RNN L-ODE-RNN refers to latent neural ODE model where the encoder is an RNN and decoder is a neural ODE proposed in [32].

L-ODE-ODE [33] proposes ODE-RNN model which generalize RNNs to have continuous-time hidden dynamics defined by ODEs. L-ODE-ODE refers to the model where the encoder is an ODE-RNN and decoder is a neural ODE.

mTAND-Full [22] proposes mTAND-Full for interpolation and classification of sparse, irregularly sampled, and multivariate time series data. mTAND-Full performs time attention mechanism to learn temporal similarity and Bidirectional RNNs to encode temporal features. Mask mechanism makes the representation of missing data and target points convenient and easy to parallel.

F Additional results

F.1 Experiments on high-dimensional synthetic data

In order to verify the scalability of NIERT on higher dimensional data, we specially constructed a synthetic 10D dataset to evaluate. In this dataset, each function is obtained by the summation of K randomly sampled 10-dimensional Gaussian functions, which can be formalized as

$$f(x) = \sum_{k=1}^K A_k \exp\left(-\frac{1}{2} \frac{(x - c_k)^2}{\sigma_k^2}\right).$$

We fix K as 5. For each Gaussian function using in each function, we uniformly sampled the center c_k from $[-1, 1]^{10}$, width σ_k from $[1, 2]$ and weight A_k from $[-1, 1]$.

We created a training set containing 256K instances and test set containing 512 cases from this function distribution. Each instance includes 64 observed points and 192 target points, which are uniformly sampled from $[-1, 1]^{10}$. On the test set, we directly evaluated the classical methods, and also evaluated the data-driven models after 100 epochs of training. We show the interpolation accuracy of these methods in the Table 8.

Approach	RBF	MIR	CNP	ANP	BANP	TFR-transformer	NIERT
Accuracy	181.744	161.474	35.623	12.578	12.077	7.465	5.496

Table 8: Interpolation accuracy ($\text{MSE} \times 10^{-4}$) on 10D test set

These results show that NIERT still maintains the best accuracy on high-dimensional data, suggesting its scalability. Noted that we only changed the input layer dimension of NIERT in order to deal with this 10-dimensional data, so the calculation cost increases by a limited margin.

F.2 More Ablation studies

The effects of different model depths

We carried out experiments on 2D NeSymReS dataset using NIERT with hyper-parameter L varying from 3 to 7. Then evaluate the models on the 2D NeSymReS test dataset. Accuracy are listed in

below Table 9. The results show that NIERT with 7 transformer layers has the best accuracy on the test set, and NIERT with 6 transformer layers has reached a comparable level. Therefore, in the experiments on NeSymReS data set, we use $L = 6$ to balance efficiency and accuracy.

Interpolation approach	Number of transformer layers L				
	3	4	5	6	7
NIERT	66.812	60.133	52.098	45.319	44.043

Table 9: Interpolation accuracy ($\text{MSE} \times 10^{-5}$) varying number of transformer layers L in NIERT on 2D NeSymReS dataset

The effects of different hidden dimensions

We also carried out experiments on 2D NeSymReS dataset using NIERT with smaller hidden dimensions d_{model} , say from 256, 128 and 64. Then evaluate the models on the 2D NeSymReS test dataset. Accuracy are listed in below Table 10. The results show that when the hidden dimension is within 512, NIERT’s interpolation accuracy is higher when the hidden dimension is larger.

In this experiment, we fix other super parameters, say model depth L as 6 and number of heads as 8.

Interpolation approach	Different hidden dimensions d_{model}			
	64	128	256	512
NIERT	106.193	72.107	51.153	45.319

Table 10: Interpolation accuracy ($\text{MSE} \times 10^{-5}$) varying hidden dimension d_{model} in NIERT on 2D NeSymReS dataset

The effects of prediction error of observed points in loss function

To verify the contribution of re-predicting values of the observed points to the interpolation task, we conducted an experiment that puts the prediction error of observed points in the loss function, i.e. only minimizes the estimation error of target points. The results are shown in Table 11 which demonstrates that only minimizing estimation error of target points make NIERT performing poorly. This indicates that re-predicting the value of observed points helps NIERT to predict the value of target points more accurately.

Loss contains prediction error of	Only target points	All points
MSE ($\times 10^{-5}$)	48.931	45.319

Table 11: Interpolation accuracy ($\text{MSE} \times 10^{-5}$) of NIERT trained with loss only containing the prediction error of the target points

The effects of partial self-attention

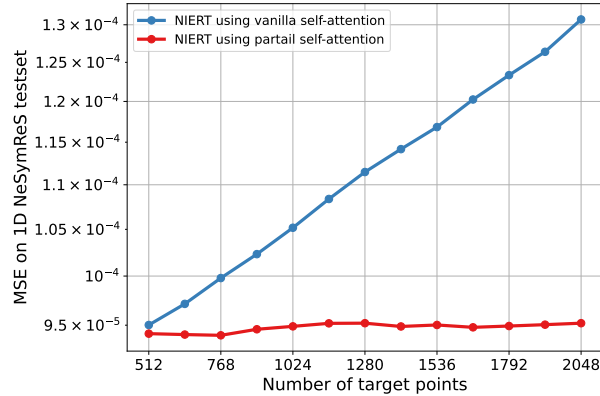


Figure 8: The robustness of NIERT to the number of target points. Here, two variants of NIERT are trained on 1D NeSymReS dataset

To verify the partial self-attention’s robustness to number of target points, Figure 7 has demonstrated that when trained with instances whose number of target points varies within [206, 246], the variant NIERT with vanilla self-attention shows poor performance for the tasks with few target points, say less than 64 target points. However, NIERT with partial self-attention performs stably without significant changes of accuracy.

As supplements to Figure 7, we examined the two variants of NIERT by evaluating them on instances whose numbers of target points are much larger than them of training instances, say, varying in [512, 2048]. As demonstrated in Figure 8, as the number of target points increases (from 512 to 2048), the interpolation error of NIERT with vanilla self-attention increases gradually. However, the interpolation accuracy of NIERT with partial self-attention is almost unchanged, and maintains at a better level.

F.3 Prediction accuracy gap between observed points and target points

Prediction accuracy on	MSE ($\times 10^{-5}$) on NeSymReS test sets			
	1D	2D	3D	4D
Observed points	1.301	4.862	3.775	2.662
Target points	8.964	45.319	77.664	72.025

Table 12: Prediction accuracy gap between observed points and target points on NeSymReS test set

We carried out an extra experiment for prediction accuracy analysis on observed points and target points. Figure 12 shows that on the observed points, the MSE of prediction is relatively smaller when compared with it of target points as expected.

F.4 More case studies

Cases from 1D & 2D NeSymReS test set

In each example of 1D interpolation task extracted from NeSymReS test set, the blue curve represents the ground-truth function while the red curves represent the interpolation functions reported by NIERT and the existing approaches.

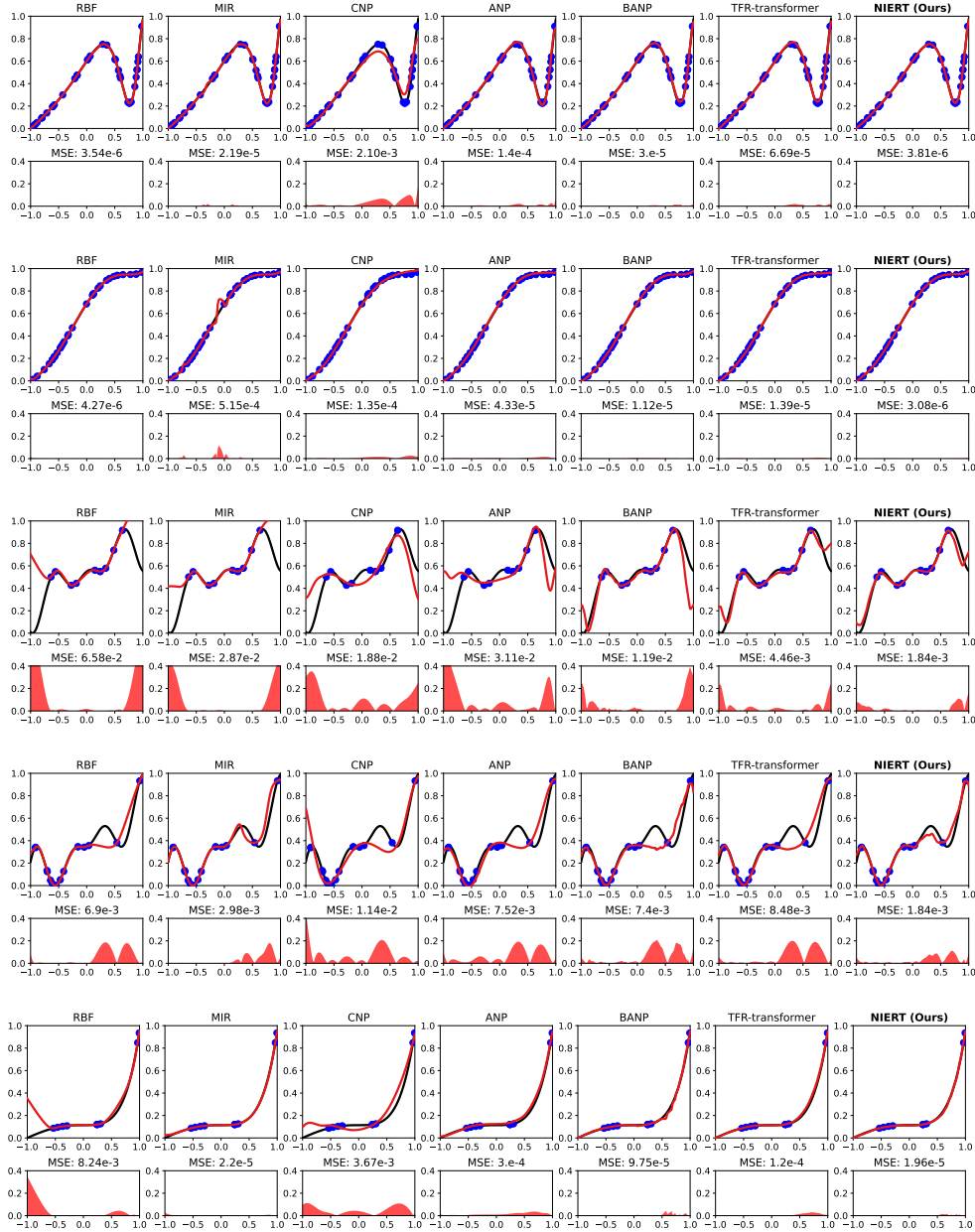


Figure 9: More cases from 1D NeSymReS test set

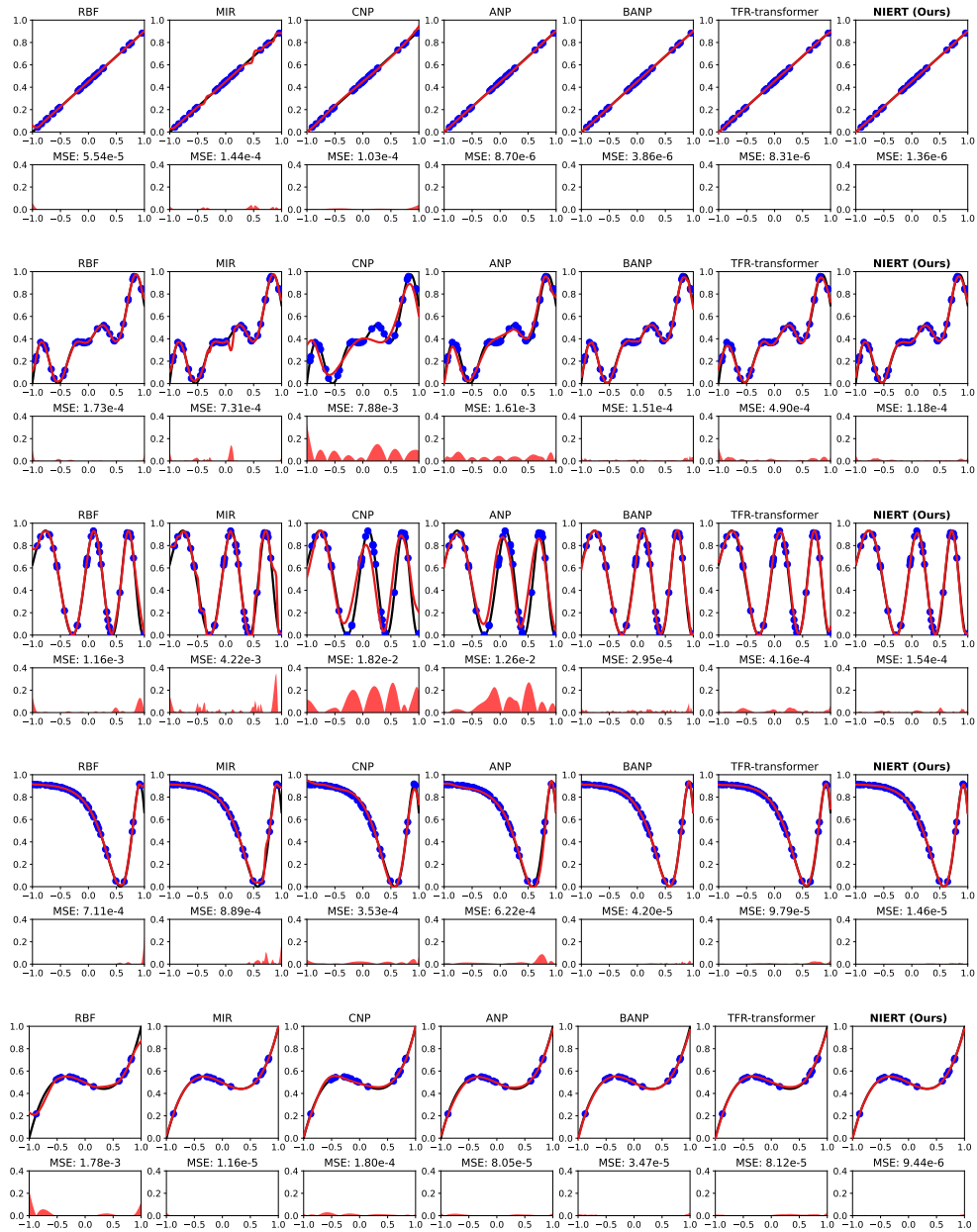


Figure 10: More cases from 1D NeSymReS test set

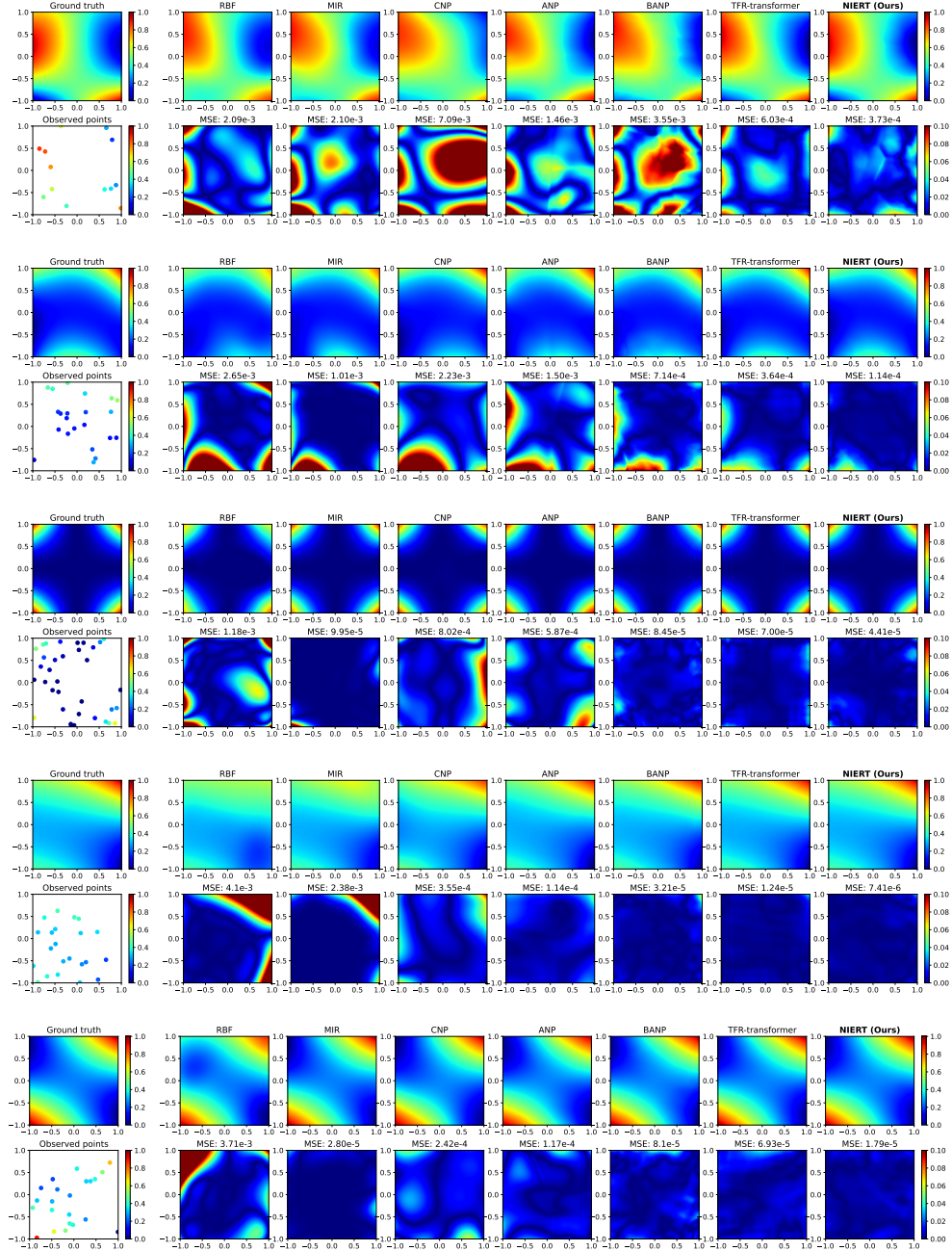


Figure 11: More cases from 2D NeSymReS test set

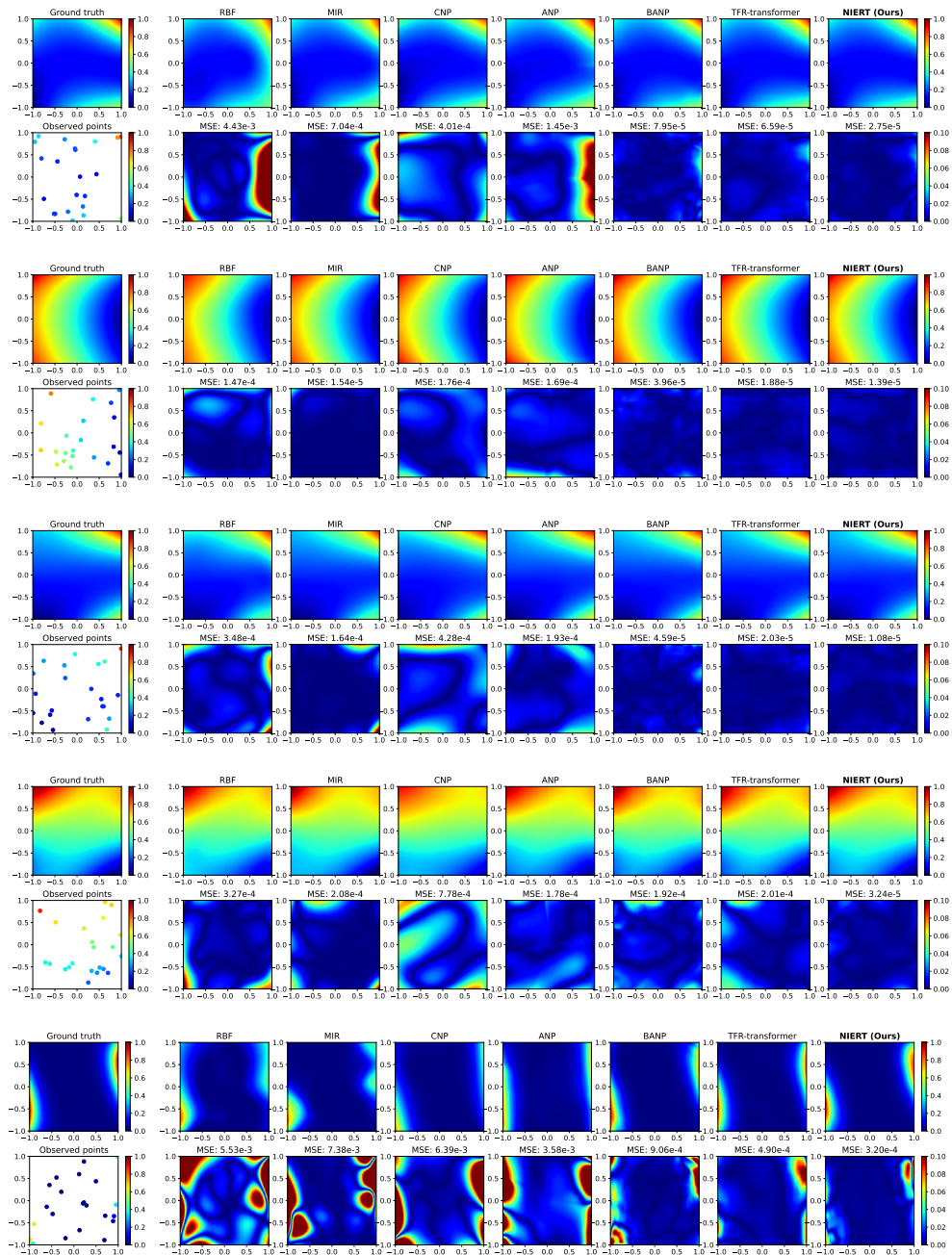


Figure 12: More cases from 2D NeSymReS test set

Cases from TFRD-ADlet

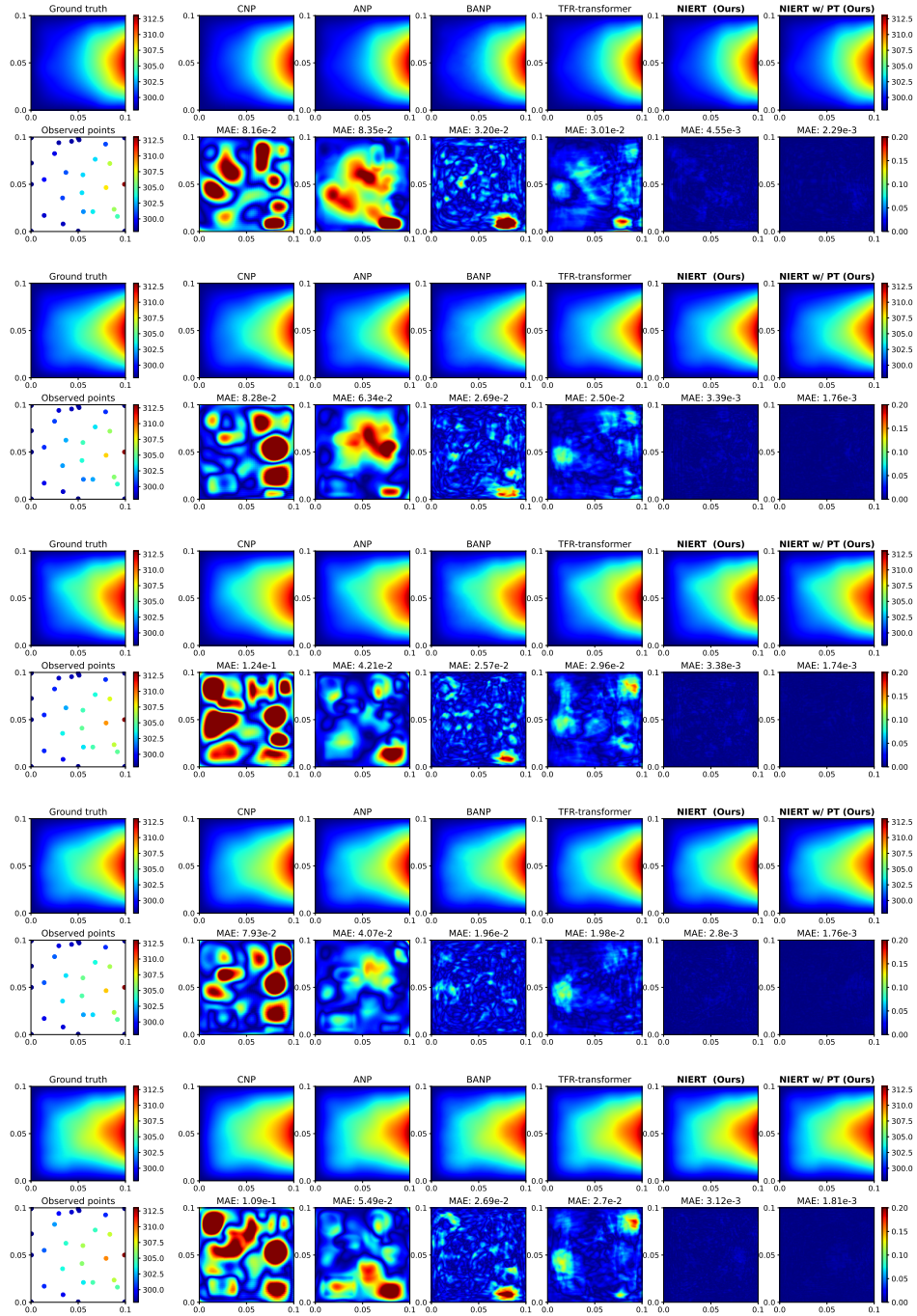


Figure 13: More cases from TFRD-ADlet test set

E.5 Contribution analysis of observed points for interpolation

As supplements to Figure 6, all observed points' attention weights extracted from the final attention layer of NIERT and TFR-transformer are visualized in Figure 14.

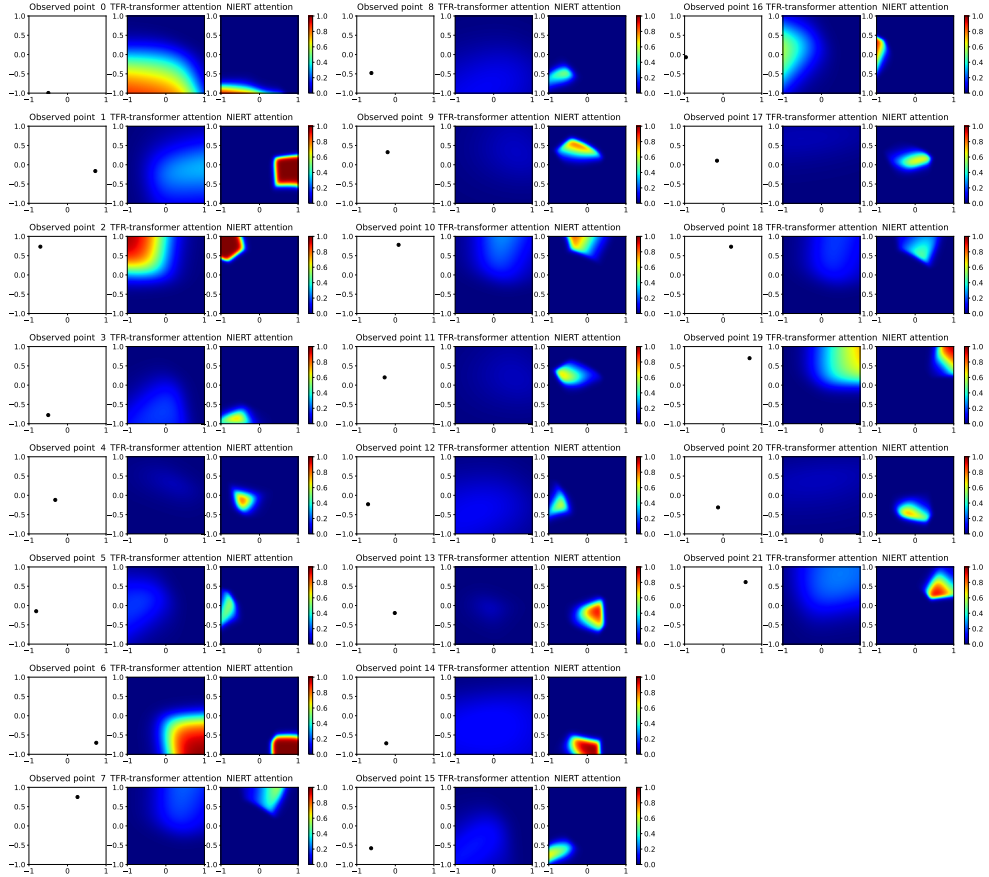


Figure 14: All observed points and the corresponding extracted attention response

The contributions by observed points are quite imbalanced using TFR-transformer. In contrast, when using NIERT, contributions by an observed point are much more local and thus targeted and all observed points have contributions to interpolation. This shows that NIERT can fully exploit the relationship between observed points and target points.